



A Simple Model for a Fluid-Filled Open-Cell Foam

UDO DÜNGER, HERBERT WEBER and HANS BUGGISCH

*Institut für Mechanische Verfahrenstechnik u. Mechanik, Bereich Angewandte Mechanik,
Universität Karlsruhe, Germany*

(Received: 29 August 1997; in final form: 20 January 1998)

Abstract. A simple microstructure model is used to describe a fluid-filled open-cell foam. In the simplest case it consists of parallel elastic plates with gaps between them, which are filled with a Newtonian fluid. We assume that the load applied to this model material is uniaxial. The constitutive equation is formulated with the pressure of the fluid as an inner variable. The model yields an evolutionary equation for the fluid pressure which itself is a field equation, that is a partial differential equation in time and space coordinates. This differential equation is solved for an instantaneously applied constant load and for a harmonically oscillating load. The solution of the differential equation, in combination with the constitutive equation leads to a relation between mean applied load and global strain of the test specimen. Finally, we obtain the creep compliance and the complex modulus of the foam material, respectively. The influence of different geometries of the foam and of different material behaviour of the matrix and fluid on the creep compliance and the complex modulus is discussed.

Key words: foam, microstructure, damping characteristic, open-cell, fluid-filled.

1. Introduction

In general, fluid-filled open-cell polymer foams are used as dampers of waves, impact loadings and vibrations. They can be applied in a broad range, for example damping of vibrations of machines, protection of sensitive goods against vibrations and impacts, and they are used in casual shoes and mattresses as well.

In order to construct fluid-filled open-cell polymer foams with desired damping characteristics, one needs to understand how the matrix material, the fluid properties, and the cavity structure influence the damping behaviour. The aim of this paper is to analyze the influence of the above parameters.

Fluid-filled open-cell foam is not a so-called 'simple material', that is the stress at a point X does not depend only on the deformation at X or the history of deformation at X . Since the fluid needs a finite time to flow out of high pressure regions into low pressure regions, the system will pass a nonequilibrium state. Therefore, the constitutive equation has to take into account long-range interactions. The well-known approach (Eringen, 1975) for a nonsimple material of higher-order gradients assumes that the stress tensor at a place X is a function of the histories of the first n gradients of deformation at X . This is not sufficient when we have pronounced long-range interactions. This is the case for open-cell foams with fluid flow interactions.

However, modelling the material as a ‘continuum with an inner fluid state variable’ also considers long-range interactions. The field equation of the inner fluid state variable is an evolutionary equation. The fluid pressure p can be taken as an inner state variable.

In the present paper, we will look at a model foam with as simple a microstructure as possible. Initially, we will consider the fluid flow through the hollow space of the matrix material in direction x . The fluid volume flow is assumed to be proportional to the loss of pressure $-\partial p/\partial x$ in this direction. For a specimen which is loaded uniaxially in x -direction the equation of state is given by

$$\sigma = \sigma(\varepsilon, p). \quad (1.1)$$

The fluid pressure p satisfies a partial differential equation in space and time coordinates. In the following this is derived for a model foam with a simple geometry.

2. Mathematical Modelling of a Porous Medium

The micromechanical model foam (Figure 1) consists of linear-elastic plates which are arranged parallel to each other. The gaps between the plates are filled with an incompressible Newtonian fluid under the pressure p . Because of the regularity of the structure, it suffices to regard a unit cell (Figure 2). The unit cell consists of two half plates and the fluid-filled space between them. Both the distance H between the middle of neighbouring plates and the width b of the plates in z -direction are assumed to be constant. This is true if the package of plates is surrounded by rigid walls, and no shear stress occurs between the walls and the plates. The actually existing shear stress can be neglected if we consider areas with sufficient distance from the boundary.

It should be mentioned that different methods exist to gain the macroscopic constitutive equations of this special porous material. On the basis of concepts from

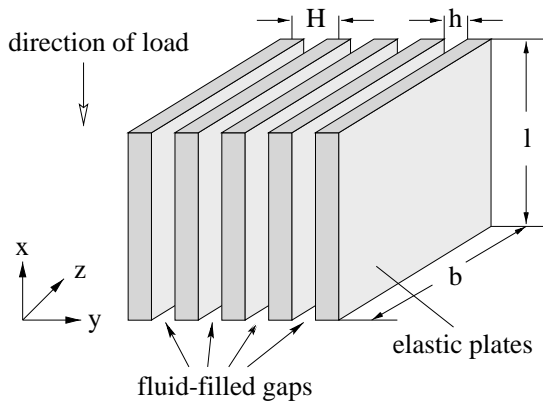


Figure 1. Micromechanical model foam.

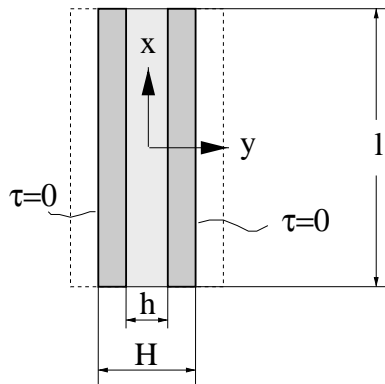


Figure 2. Unit cell.

continuum mechanics, Biot's theory of poroelasticity (Biot, 1956; Detournay and Cheng, 1993) could be applied, or the theory of mixtures extended by the concept of volume fractions (de Boer *et al.*, 1991). Because of the periodic microstructure, it would also be possible to apply homogenization techniques like those which are used in the mechanics of composite materials (Coussy, 1991). With the material under consideration, however, a difficulty arises when such theories are used. This is due to the fact that, in the direction perpendicular to the plates, the solid is not interconnected. Therefore, it is difficult to find the proper stress-strain relation for this direction. It seems to be easier to treat this problem in an elementary manner.

For the following considerations, we assume that inertia effects can be neglected, and that the strain is small. The shear deformation will not be taken into account. We will investigate two different cases. First, we consider the fluid flowing in the direction of the applied load. As a second case, we analyze the fluid flowing perpendicular to the direction of the applied load. In the first case the load is applied stress controlled, and, in the second one, it is applied strain controlled. This is done for the simplicity of the averaging integration of the constitutive equations.

2.1. FLOW PARALLEL TO THE DIRECTION OF AN APPLIED LOAD

Here, we will calculate the averaged strain $\bar{\varepsilon}$ in x -direction in the case when a normal stress σ in x -direction is applied to the elastic plates by means of rigid end plates (Figure 3). Owing to the applied load, the fluid flows in x -direction.

The strain ε_y in y -direction and the strain ε in x -direction of the linear-elastic plates depend on both the fluid pressure p within the gaps and the stress σ in x -direction inside the plates.

Hooke's law for plain strain yields

$$\varepsilon = \frac{1 - \nu^2}{E} \sigma + \frac{\nu (1 + \nu)}{E} p, \quad (2.1)$$

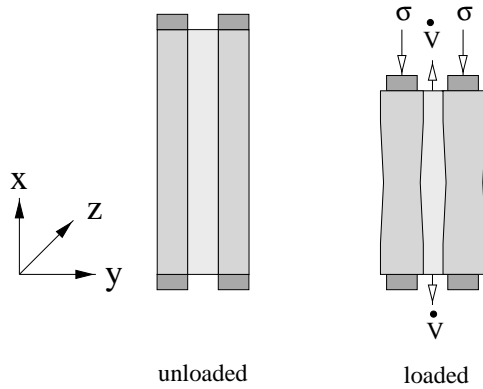


Figure 3. Loaded and unloaded plates, flow parallel to an applied normal stress.

$$\varepsilon_y = -\frac{1-\nu^2}{E} p - \frac{\nu(1+\nu)}{E} \sigma, \quad (2.2)$$

with E being Young's modulus and ν Poisson's ratio of the plate material. Let h_0 be the distance of the unloaded plates and δh the small change of gap width due to the applied strain. Then the gap width under load is

$$h(x, t) = h_0 + \delta h(x, t). \quad (2.3)$$

Therefore, the strain of a plate in y -direction is

$$\varepsilon_y = -\frac{\delta h}{H - h_0}, \quad (2.4)$$

and, with (2.2), the change δh of the gap width can be written in the form

$$\delta h = (H - h_0) \left[\frac{1-\nu^2}{E} p + \frac{\nu(1+\nu)}{E} \sigma \right]. \quad (2.5)$$

The flow of fluid between two plates caused by the applied stress is assumed to be quasi-stationary. Furthermore, we assume the change of the plate thickness δh to be small compared to the plate thickness, that is the stream lines are roughly straight-lined and parallel to each other. With these assumptions the Navier–Stokes equations lead to Darcy's law, and the averaged velocity v in x -direction depends on the fluid viscosity η , the permeability coefficient K and the loss of pressure $-\partial p/\partial x$. The velocity v , that is the volume flow \dot{V} referred to the area $b \cdot h$, is given by

$$\frac{\dot{V}}{bh} = v = \frac{K}{\eta} \left(-\frac{\partial p}{\partial x} \right). \quad (2.6)$$

If we assume furthermore that the length b of the plates is much larger than the gap width h , then K is the permeability coefficient of two flat plates and is given by

$$K = \frac{1}{12} h^2. \quad (2.7)$$

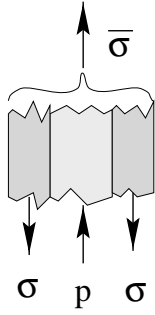


Figure 4. Averaged normal stress.

A change in the distance h of two plates, that is a volume change of the fluid-filled space, leads to a flow of the incompressible fluid. The balance of the fluid volume yields

$$\frac{\partial(\dot{V}/b)}{\partial x} = -\frac{\partial h}{\partial t} - h \frac{\partial \varepsilon}{\partial t}. \tag{2.8}$$

Until now we have not taken into account that, due to the fluid flow, a shear stress τ_f , interacting at the boundary between fluid and matrix material, arises. The equilibrium of forces at a unit cell (Figure 4) yields

$$(H - h)\sigma - p h = \bar{\sigma} H. \tag{2.9}$$

Here, $\bar{\sigma}$ denotes the averaged stress in x -direction. The pressure term in (2.9) represents the effect of the shear stress τ_f . Instead of the shear stress τ_f acting at the surface area, we can imagine a volume force inside every plate. This ‘pseudo volume force’ has the same effect as the shear stress τ_f , as can be derived from differentiating (2.9) and noting that pressure drop and shear stress are proportional:

$$\frac{\partial \sigma}{\partial x} = \underbrace{\frac{h}{H - h} \frac{\partial p}{\partial x}}_{\text{pseudo volume force}} \propto \frac{\tau_f}{H - h}. \tag{2.10}$$

The constitutive equation of the model foam is now obtained by substitution of the equilibrium equation (2.9) into Hooke’s law (2.1), linearizing with respect to p , σ and δh , and by a subsequent integration over the height of the plates:

$$\bar{\varepsilon} = A_{\parallel} \bar{\sigma} + B_{\parallel} \frac{1}{l} \int_{-l/2}^{l/2} p \, dx \tag{2.11}$$

with the constants

$$A_{\parallel} = \frac{1 - \nu^2}{E (1 - h_0/H)}, \quad B_{\parallel} = \frac{1 + \nu}{E (1 - h_0/H)} \left[\nu + (1 - 2\nu) \frac{h_0}{H} \right]. \tag{2.12}$$

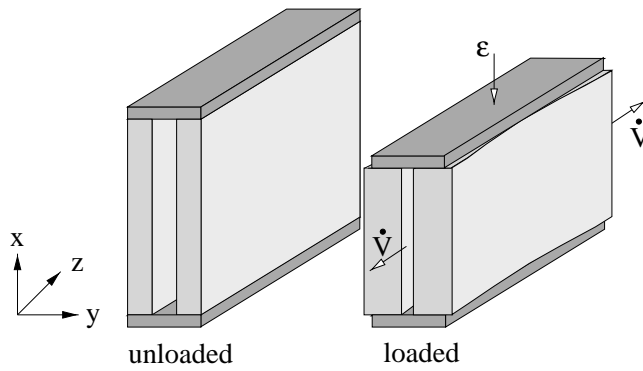


Figure 5. Loaded and unloaded plates, flow perpendicular to an applied strain.

Finally, we obtain the partial differential equation of the inner variable p from (2.1), (2.2) and (2.5)–(2.9). Neglecting nonlinear terms results in

$$a_{\parallel} \frac{\partial^2 p}{\partial x^2} - \frac{\partial p}{\partial t} = k_{\parallel} \frac{d\bar{\sigma}}{dt}, \quad (2.13)$$

where

$$a_{\parallel} = \frac{E h_0^2}{12 \eta} \frac{(h_0/H)(1 - h_0/H)}{(1 + \nu)[1 - \nu - 2(1 - 2\nu)(h_0/H)(1 - h_0/H)]}, \quad (2.14)$$

$$k_{\parallel} = \frac{\nu + (1 - 2\nu)(h_0/H)}{1 - \nu - 2(1 - 2\nu)(h_0/H)(1 - h_0/H)}.$$

2.2. FLOW PERPENDICULAR TO THE DIRECTION OF AN APPLIED LOAD

We now calculate the averaged stress $\bar{\sigma}$ in x -direction for the case where rigid end plates apply a strain ε in x -direction to the elastic plates and the fluid between them (Figure 5). Owing to the applied strain and the boundary conditions, the fluid flows in z -direction perpendicular to the applied load.

In principle, the derivation of both the constitutive equation and the partial differential equation for p is analogous to the first case in 2.1, but there are some important differences.

The state of strain is now three-dimensional. Hooke's law yields

$$\varepsilon = \frac{1}{E} [\sigma - \nu(\sigma_z - p)], \quad (2.15)$$

$$\varepsilon_y = -\frac{1}{E} [p + \nu(\sigma + \sigma_z)], \quad (2.16)$$

$$\varepsilon_z = -\frac{1}{E} [\sigma_z - \nu(\sigma - p)]. \quad (2.17)$$

Insertion of (2.16) into (2.4) yields

$$\delta h = \frac{H - h_0}{E} [(1 - \nu^2) p + (\nu + \nu^2) \sigma + \nu E \varepsilon_z]. \quad (2.18)$$

The fluid velocity v_z in z -direction is given by

$$\frac{\dot{V}}{lh} = v_z = \frac{K}{\eta} \left(-\frac{\partial p}{\partial z} \right). \quad (2.19)$$

Assuming that the height l of the plates is much larger than the gap width h , the permeability coefficient K again coincides with the permeability coefficient of flat plates (2.7). The balance of fluid volume yields

$$\frac{\partial(\dot{V}/l)}{\partial z} = -\frac{\partial h}{\partial t} - h \left(\frac{\partial \varepsilon}{\partial t} + \frac{\partial \varepsilon_z}{\partial t} \right). \quad (2.20)$$

The equilibrium of forces in z -direction at a fluid element shows that the shear stress τ_f at the boundary between fluid and matrix material is proportional to the pressure loss $-\partial p/\partial z$:

$$\tau_f = -\frac{h}{2} \frac{\partial p}{\partial z}. \quad (2.21)$$

The equilibrium of forces in z -direction at an element of the matrix material leads to the equation

$$\frac{\partial \sigma_z}{\partial z} = \frac{2}{H - h} \tau_f = \frac{h}{H - h} \frac{\partial p}{\partial z}. \quad (2.22)$$

If the fluid pressure $p = 0$, there will be no strain ε_z in z -direction. This results, with (2.15) and (2.17), in the following relations:

$$\begin{aligned} \sigma &= \frac{\nu(2h - H)}{H - h} p + \frac{1}{1 - \nu^2} \varepsilon E, \\ \sigma_z &= \frac{h}{H - h} p + \frac{\nu}{1 - \nu^2} \varepsilon E. \end{aligned} \quad (2.23)$$

The linearized average stress $\bar{\sigma}$ in x -direction is defined as

$$\bar{\sigma} = \frac{1}{b} \int_{-b/2}^{b/2} \left[\left(1 - \frac{h_0}{H} \right) \sigma - \frac{h_0}{H} p \right] dz. \quad (2.24)$$

Substituting (2.23) into (2.24), and neglecting nonlinear terms, we obtain the constitutive equation

$$\bar{\sigma} = A_{\perp} \bar{\varepsilon} + B_{\perp} \frac{1}{b} \int_{-b/2}^{b/2} p dz \quad (2.25)$$

with

$$A_{\perp} = \left(\frac{1 - h_0/H}{1 - \nu^2} \right) E, \quad B_{\perp} = -(1 - 2\nu) \frac{h_0}{H} - \nu. \quad (2.26)$$

Finally, we obtain the partial differential equation of the inner variable p from (2.7), (2.15), (2.17)–(2.20) and (2.23). Neglecting nonlinear terms results in

$$a_{\perp} \frac{\partial^2 p}{\partial x^2} - \frac{\partial p}{\partial t} = k_{\perp} \frac{d\bar{\epsilon}}{dt}, \quad (2.27)$$

where

$$a_{\perp} = a_{\parallel} = \frac{E h_0^2}{12 \eta} \frac{(h_0/H)(1 - h_0/H)}{(1 + \nu)[1 - \nu - 2(1 - 2\nu)(h_0/H)(1 - h_0/H)]}, \quad (2.28)$$

$$k_{\perp} = \frac{[\nu + (1 - 2\nu)h_0/H](1 - h_0/H)}{(1 - \nu^2)[1 - \nu - 2(1 - 2\nu)(h_0/H)(1 - h_0/H)]} E.$$

3. Solution of the Partial Differential Equations

The partial differential Equations (2.13) and (2.27) are of the same type. Subsequently, the solution of (2.13) is given for both an instantaneously and a sinusoidally applied load.

3.1. SOLUTION FOR AN INSTANTANEOUSLY APPLIED LOAD

Let us consider the case where the load $\bar{\sigma}$ is linearly increased from 0 to $\bar{\sigma}_0$ in the time interval $[0, \delta t_0]$, and then kept constant at the value $\bar{\sigma}_0$.

The differential Equation (2.13) can then be written as

$$a_{\parallel} \frac{\partial^2 p}{\partial x^2} = \frac{\partial p}{\partial t} + k_{\parallel} \frac{\bar{\sigma}_0}{\delta t_0} \quad \text{for } 0 < t < \delta t_0, \quad (3.1)$$

$$a_{\parallel} \frac{\partial^2 p}{\partial x^2} = \frac{\partial p}{\partial t} \quad \text{for } t > \delta t_0.$$

An instantaneously applied stress $\bar{\sigma}$ will lead to an abruptly increased constant fluid pressure. Therefore, the initial condition of the fluid pressure immediately after an applied jump of stress can be written as

$$p(\delta t_0) = -k_{\parallel} \bar{\sigma}_0 \quad \text{for } \delta t_0 \rightarrow 0. \quad (3.2)$$

We assume the fluid pressure at the end of the plates in x -direction to be zero. This gives the boundary conditions

$$p(x = \frac{1}{2}l, t) = p(x = -\frac{1}{2}l, t) = 0. \quad (3.3)$$

With these boundary conditions and the initial condition (3.2), we obtain the following Fourier series as a solution of the differential equation (2.13) for the case of a jump of stress:

$$p(x, t) = -k_{\parallel} \bar{\sigma}_0 \frac{4}{\pi} \sum_{n=1}^{\infty} \left\{ \frac{(-1)^{n+1}}{2n-1} \cdot \frac{\cos[(2n-1)\pi(x/l)]}{\exp[\pi^2(a_{\parallel}/l^2)(2n-1)^2 t]} \right\}. \quad (3.4)$$

3.2. SOLUTION FOR A SINUSOIDALLY APPLIED LOAD

Now we consider a sinusoidally applied load

$$\bar{\sigma} = \bar{\sigma}_0 \sin \omega t \quad (3.5)$$

with the angular frequency ω . The approach

$$p(x, t) = f(x) \sin \omega t + g(x) \cos \omega t \quad (3.6)$$

and the same boundary conditions as before (fluid pressure at the ends of the plates = ambient pressure = 0) give the following solution of the differential equation:

$$\begin{aligned} p(x, t) = & \frac{k_{\parallel} \bar{\sigma}_0}{\sin^2(\frac{1}{2} l K_{\parallel}) \sinh^2(\frac{1}{2} l K_{\parallel}) + \cos^2(\frac{1}{2} l K_{\parallel}) \cosh^2(\frac{1}{2} l K_{\parallel})} \times \\ & \times \{ [-\sin^2(\frac{1}{2} l K_{\parallel}) \sinh^2(\frac{1}{2} l K_{\parallel}) - \\ & - \cos^2(\frac{1}{2} l K_{\parallel}) \cosh^2(\frac{1}{2} l K_{\parallel}) + \\ & + \sin(x K_{\parallel}) \sinh(x K_{\parallel}) \sin(\frac{1}{2} l K_{\parallel}) \sinh(\frac{1}{2} l K_{\parallel}) + \\ & + \cos(x K_{\parallel}) \cosh(x K_{\parallel}) \cos(\frac{1}{2} l K_{\parallel}) \cosh(\frac{1}{2} l K_{\parallel})] \sin \omega t + \\ & + [\sin(x K_{\parallel}) \sinh(x K_{\parallel}) \cos(\frac{1}{2} l K_{\parallel}) \cosh(\frac{1}{2} l K_{\parallel}) - \\ & - \cos(x K_{\parallel}) \cosh(x K_{\parallel}) \sin(\frac{1}{2} l K_{\parallel}) \sinh(\frac{1}{2} l K_{\parallel})] \cos \omega t \} \end{aligned} \quad (3.7)$$

with

$$K_{\parallel} = \sqrt{\frac{\omega}{2a_{\parallel}}}. \quad (3.8)$$

4. Results

4.1. FLOW PARALLEL TO THE DIRECTION OF AN APPLIED LOAD

4.1.1. Material Behaviour for an Instantaneously Applied Load

The creep law, that is the relation between the averaged strain $\bar{\varepsilon}$ and an instantaneously applied load $\bar{\sigma}_0$, is obtained by inserting (3.4) into (2.11):

$$\begin{aligned}\bar{\varepsilon}(t) &= \left[A_{\parallel} - \frac{8}{\pi^2} B_{\parallel} k_{\parallel} \sum_{n=1}^{\infty} \frac{\exp[-\pi^2(a_{\parallel}/l^2)(2n-1)^2 t]}{(2n-1)^2} \right] \bar{\sigma}_0 \\ &= D(t) \bar{\sigma}_0.\end{aligned}\quad (4.1)$$

The term $D(t)$ is called creep compliance. For the initial value ($t \rightarrow 0$) and for the equilibrium value ($t \rightarrow \infty$) of $D(t)$ we get

$$\begin{aligned}D(t \rightarrow 0) &= A_{\parallel} - B_{\parallel} k_{\parallel}, \\ D(t \rightarrow \infty) &= A_{\parallel}.\end{aligned}\quad (4.2)$$

4.1.2. Material Behaviour for a Sinusoidally Applied Load

In the case of a sinusoidally applied load (3.5), we have to insert the solution (3.7) of the partial differential Equation (2.13) into the constitutive Equation (2.11). This gives the following expression for the averaged sinusoidal strain:

$$\bar{\varepsilon} = \bar{\sigma}_0 \sqrt{C_{1\parallel}^2 + C_{2\parallel}^2} \sin(\omega t + \varphi) \quad (4.3)$$

with

$$\begin{aligned}C_{1\parallel} &= A_{\parallel} - B_{\parallel} k_{\parallel} + \frac{B_{\parallel} k_{\parallel}}{l K_{\parallel}} \times \\ &\quad \times \frac{\sinh(\frac{1}{2} l K_{\parallel}) \cosh(\frac{1}{2} l K_{\parallel}) + \sin(\frac{1}{2} l K_{\parallel}) \cos(\frac{1}{2} l K_{\parallel})}{[\sin(\frac{1}{2} l K_{\parallel}) \sinh(\frac{1}{2} l K_{\parallel})]^2 + [\cos(\frac{1}{2} l K_{\parallel}) \cosh(\frac{1}{2} l K_{\parallel})]^2},\end{aligned}\quad (4.4)$$

$$C_{2\parallel} = \frac{B_{\parallel} k_{\parallel}}{l K_{\parallel}} \cdot \frac{\sin(\frac{1}{2} l K_{\parallel}) \cos(\frac{1}{2} l K_{\parallel}) - \sinh(\frac{1}{2} l K_{\parallel}) \cosh(\frac{1}{2} l K_{\parallel})}{[\sin(\frac{1}{2} l K_{\parallel}) \sinh(\frac{1}{2} l K_{\parallel})]^2 + [\cos(\frac{1}{2} l K_{\parallel}) \cosh(\frac{1}{2} l K_{\parallel})]^2}.\quad (4.5)$$

The loss angle φ is given by

$$\tan \varphi = \frac{C_{2\parallel}}{C_{1\parallel}}, \quad (4.6)$$

and the dynamic modulus E_{dyn} is given by

$$E_{\text{dyn}} = \frac{\bar{\sigma}_0}{\bar{\varepsilon}_0} = 1/\sqrt{C_{1\parallel}^2 + C_{2\parallel}^2}.\quad (4.7)$$

The theoretical treatment predicts that the dynamic modulus E_{dyn} and the tangent of the loss angle, $\tan \varphi$, are functions of the ratio h_0/H , Poisson's ratio ν of the linear-elastic plates and a certain dimensionless quantity. This quantity Π_{\parallel} is the following function of the angular frequency ω , the viscosity of the fluid η , Young's modulus E of the linear-elastic plates and the ratio of the fluid path length l to the gap length h_0 :

$$\Pi_{\parallel} = \omega \left(\frac{l}{h_0} \right)^2 \frac{\eta}{E}. \tag{4.8}$$

For small values of the dimensionless quantity Π_{\parallel} , the dynamic modulus E_{dyn} , denoted E_{stat} , is equal to the reciprocal of the creep compliance for large values of t :

$$E_{\text{dyn}} (\Pi_{\parallel} \rightarrow 0) = E_{\text{stat}} = \frac{1}{D(t \rightarrow \infty)} = \frac{1}{A_{\parallel}}. \tag{4.9}$$

For very large values of the dimensionless quantity Π_{\parallel} , the dynamic modulus E_{dyn} is equal to the reciprocal of the short-time creep compliance:

$$E_{\text{dyn}} (\Pi_{\parallel} \rightarrow \infty) = \frac{1}{D(t \rightarrow 0)} = \frac{1}{A_{\parallel} - B_{\parallel} k_{\parallel}}. \tag{4.10}$$

Thus, it will be sufficient to look at the material behaviour of a harmonically applied load.

The tangent of the loss angle is a measure of the energy dissipation per cycle. At low values of Π_{\parallel} , the tangent of the loss angle increases with the quantity Π_{\parallel} , due to the fluid flow relative to the matrix. The fluid flow at higher values of Π_{\parallel} is more and more in phase with the applied load, and the tangent of the loss angle decreases. The fluid flow is negligible at high values of Π_{\parallel} , and the $\tan \varphi$ tends towards zero. This qualitative behaviour is shown in Figures 6 and 8. Furthermore, in Figure 6 it is shown that increasing values of Poisson's ratio ν cause a higher energy dissipation. The energy dissipation also increases with increasing ratio h_0/H (Figure 8), which can be interpreted as the portion of the fluid volume.

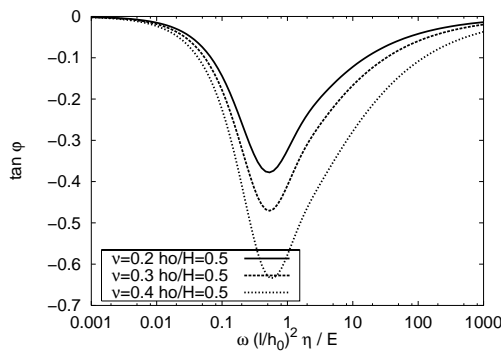


Figure 6. Tangent of the loss angle versus Π_{\parallel} , variation of ν .

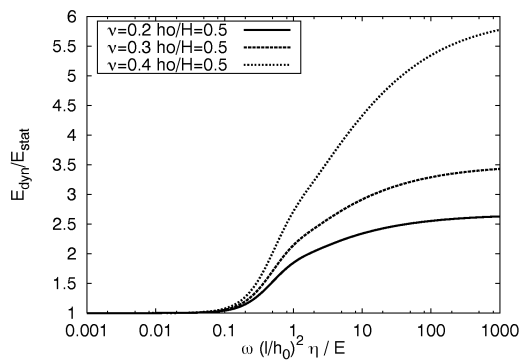


Figure 7. Dynamic modulus with respect to the static modulus versus Π_{\parallel} , variation of ν .

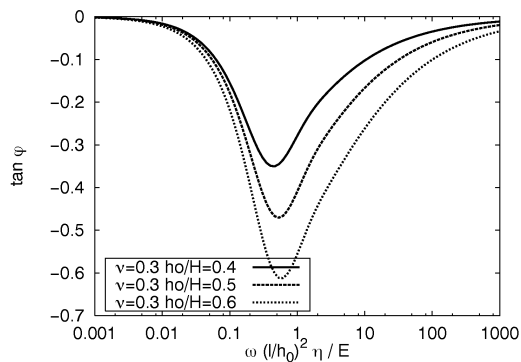


Figure 8. Tangent of the loss angle versus Π_{\parallel} , variation of h_0/H .

The fluid flow relative to the matrix causes the dynamic modulus to increase with the quantity Π_{\parallel} . At high values of Π_{\parallel} , the fluid flow is negligible, and the incompressible fluid acts as a hindering for the lateral strain. This means that the dynamic modulus increases with increasing values of Π_{\parallel} , and tends towards a maximum at high values of Π_{\parallel} . This behaviour is shown in Figure 7 and Figure 9. The dynamic modulus, with respect to the static modulus, increases with increasing values of Poisson's ratio ν (Figure 7), and also increases with increasing portion of the fluid volume (Figure 9).

It is worth mentioning that the Poisson's ratio has a considerable effect on the material behaviour in the case of the flow being parallel to the direction of an applied load. This effect should not be neglected. The qualitative material behaviour of our model is the same as (Rusch, 1965) predicted with his model, but he did not take into account the effect of compressible matrix material. In addition, we can omit some assumptions which (Rusch, 1965) needed to set up his model.

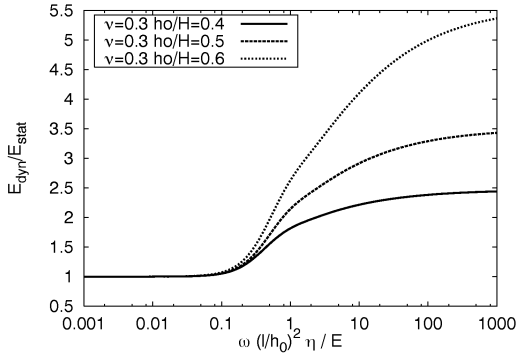


Figure 9. Dynamic modulus with respect to the static modulus versus Π_{\parallel} , variation of h_0/H .

4.2. FLOW PERPENDICULAR TO THE DIRECTION OF AN APPLIED LOAD

4.2.1. Material Behaviour for a Sinusoidally Applied Strain

In the case of a sinusoidally applied strain $\bar{\varepsilon}_0 \sin \omega t$, the solution of the partial differential Equation (2.27), inserted into the constitutive Equation (2.25), gives the following expression for the averaged stress:

$$\bar{\sigma} = \bar{\varepsilon}_0 \sqrt{C_{1\perp}^2 + C_{2\perp}^2} \sin(\omega t + \varphi) \quad (4.11)$$

with

$$C_{1\perp} = A_{\perp} - B_{\perp} k_{\perp} + \frac{B_{\perp} k_{\perp}}{b K_{\perp}} \times \frac{\sinh(\frac{1}{2} b K_{\perp}) \cosh(\frac{1}{2} b K_{\perp}) + \sin(\frac{1}{2} b K_{\perp}) \cos(\frac{1}{2} b K_{\perp})}{[\sin(\frac{1}{2} b K_{\perp}) \sinh(\frac{1}{2} b K_{\perp})]^2 + [\cos(\frac{1}{2} b K_{\perp}) \cosh(\frac{1}{2} b K_{\perp})]^2}, \quad (4.12)$$

$$C_{2\perp} = \frac{B_{\perp} k_{\perp}}{b K_{\perp}} \cdot \frac{\sin(\frac{1}{2} b K_{\perp}) \cos(\frac{1}{2} b K_{\perp}) - \sinh(\frac{1}{2} b K_{\perp}) \cosh(\frac{1}{2} b K_{\perp})}{[\sin(\frac{1}{2} b K_{\perp}) \sinh(\frac{1}{2} b K_{\perp})]^2 + [\cos(\frac{1}{2} b K_{\perp}) \cosh(\frac{1}{2} b K_{\perp})]^2}, \quad (4.13)$$

$$K_{\perp} = \sqrt{\frac{\omega}{2a_{\perp}}}. \quad (4.14)$$

In this case, the loss angle φ is given by

$$\tan \varphi = \frac{C_{2\perp}}{C_{1\perp}}, \quad (4.15)$$

and the dynamic modulus E_{dyn} follows from

$$E_{\text{dyn}} = \frac{\bar{\sigma}_0}{\bar{\varepsilon}_0} = \sqrt{C_{1\perp}^2 + C_{2\perp}^2}. \quad (4.16)$$

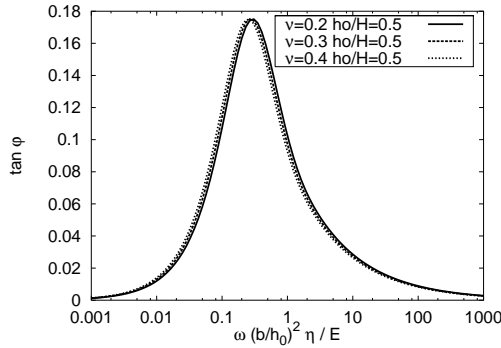


Figure 10. Tangent of the loss angle versus Π_{\perp} , variation of ν .

The dynamic modulus E_{dyn} and the tangent of the loss angle, $\tan \varphi$, are again functions of the ratio h_0/H , Poisson’s ratio ν of the linear-elastic plates and a certain dimensionless quantity. This quantity Π_{\perp} is analogous to the quantity Π_{\parallel} , but the ratio of the fluid path length to the gap length is now given by b/h_0 :

$$\Pi_{\perp} = \omega \left(\frac{b}{h_0} \right)^2 \frac{\eta}{E}. \tag{4.17}$$

For small values of the dimensionless quantity Π_{\perp} , the dynamic modulus E_{dyn} , denoted E_{stat} , is

$$E_{\text{dyn}} (\Pi_{\perp} \rightarrow 0) = E_{\text{stat}} = A_{\perp}. \tag{4.18}$$

For very large values of the dimensionless quantity Π_{\perp} , the dynamic modulus E_{dyn} is given by

$$E_{\text{dyn}} (\Pi_{\perp} \rightarrow \infty) = A_{\perp} - B_{\perp} k_{\perp}. \tag{4.19}$$

The qualitative material behaviour when the flow is perpendicular to the load is similar to the behaviour of the case where the flow is parallel to the load (Figures

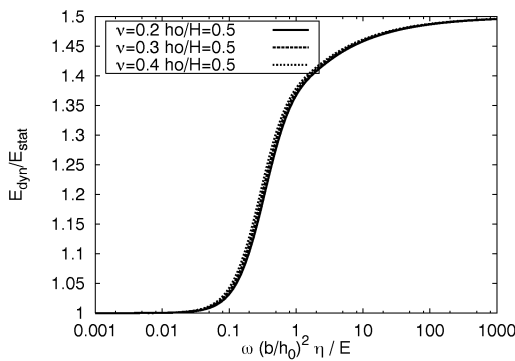


Figure 11. Dynamic modulus with respect to the static modulus versus Π_{\perp} , variation of ν .

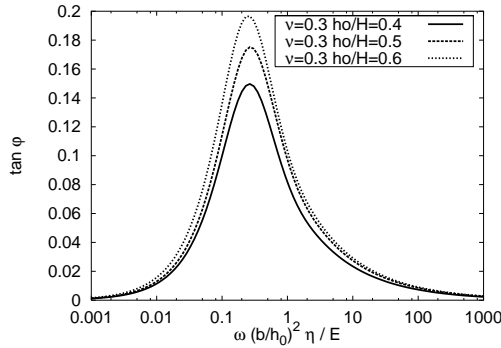


Figure 12. Tangent of the loss angle versus Π_{\perp} , variation of h_0/H .

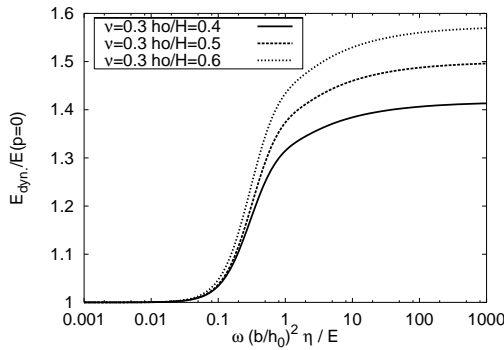


Figure 13. Dynamic modulus with respect to the static modulus versus π_{\perp} , variation of h_0/H .

10–13). The maximum energy dissipation per cycle, when the flow is perpendicular to the load, is considerably lower than the maximum energy dissipation of the first case. However, now the influence of Poisson’s ratio on both, the tangent of the loss angle (Figure 10) and the dynamic modulus (Figure 11), is negligible. Increasing values of the fluid volume portion h_0/H again cause a higher energy dissipation (Figure 12) and higher values of the dynamic modulus (Figure 13).

5. Conclusion

The presented micromechanical model of a fluid-filled open-cell foam is appropriate to describe the damping behaviour resulting from fluid flow during deformation. Furthermore, the model yields the parameters upon which the damping behaviour depends. This cannot be found by using macroscopic continuum approaches, and, with this understanding, it is possible to construct fluid-filled open-cell polymer foams with desired damping characteristics.

The parameters on which the damping behaviour depends, are the Poisson’s ratio ν , the fluid volume portion h_0/H and a dimensionless quantity. When the

load is applied parallel to the direction of the fluid flow, the quantity is given by $\omega (l/h_0)^2 \eta/E$, and, when the load is applied perpendicular to the direction of the fluid flow, the quantity is given by $\omega (b/h_0)^2 \eta/E$.

References

- Biot, M. A.: 1956, General solutions of the equations of elasticity and consolidation for a porous material, *J. Appl. Mech. Trans. ASME* **78**, 91–96.
- Coussy, O.: 1991, *Méchanique des Milieux Poreux*, Editions Technip, Paris.
- de Boer, R., Ehlers, W., Kowalski, S. and Plischka, J.: 1991, Porous media: A survey of different approaches, *Forschungsberichte aus dem Fachgebiet Bauwesen* 54, Univ.-GH Essen.
- Detournay, E. and Cheng, A. H.-D.: 1993, *Fundamentals of Poroelasticity*, *Comprehensive Rock Engineering*, In: J. Hudson (ed.), Pergamon Press, Oxford.
- Eringen, A. C.: 1975, *Continuum Physics*, Vol. II, Academic Press, New York.
- Rusch, K. C.: 1965, Dynamic behaviour of flexible open-cell foams, PhD Thesis, The University of Akron, pp. 28–36.